Sensing and Bio-Sensing Research 30 (2020) 100378

Contents lists available at ScienceDirect

Sensing and Bio-Sensing Research

journal homepage: www.elsevier.com/locate/sbsr

Design of a low cost, double triangle, piezoelectric sensor for respiratory monitoring applications

Amir Panahi, Alireza Hassanzadeh*, Ali Moulavi

Department of Electrical Engineering, Shahid Beheshti University, Tehran, Iran

ARTICLE INFO

Keywords:
Respiratory monitoring
Polyvinylidene fluoride (PVDF)
Piezoelectric sensor
Triangular structure
COVID-19
Charge amplifier.

ABSTRACT

In this paper, a novel piezoelectric sensor is presented for patient's breath monitoring applications. Breath rate monitoring is important especially for the new coronavirus patients. In this work, a piezoelectric sensor is designed in the form of a vertex-attached triangular beam made of Polyvinylidene fluoride (PVDF) and Polydimethylsiloxane (PDMS). It exploits chest displacement to distinguish breathing vibrations. The device shape and dimensions have been designed for low frequency operation. The output respiration signal is amplified using a low power charge amplifier circuit. The sensor can be placed in a vest and fastened as a belt, or be attached to the chest by a tape. A low pass filter is used to eliminate the noise from the environment and body movement. Among the most important features are high accuracy, low resonance frequency to distinguish chest movement, low weight, low cost, portability, and reliability. Simulation of the designed sensor using COMSOL shows output voltage of 1 V at breathing frequency of 0.2 Hz.

1. Introduction

Breath monitoring is one of the vital signs used for critical patient care. Design of a versatile sensor to monitor breathing is an important task, which has not been considered widely in the past. Long term or manual breath monitoring is difficult and needs several professional and trained personnel. It has been shown that a sudden change in the heartbeat and abnormal breathing indicate the onset and progression of diseases such as sudden cardiac death, asphyxia (choking), sleep apnea, etc. [2–5]. Breathing rates above 30 breaths per minute can be a sign of the new coronavirus (COVID-19) [6]. Therefore, exploring a system to monitor breathing is of a great importance. Normal respiration rate for an adult is about 12 to 20 breaths per minute. Higher than 25, as well as lower than 12, breaths per minute are symptoms of diseases [1]. Respiration rate frequency ranges from 0.1 to 0.5 Hz. In the past, there have been different methods to monitor breathing, including listening to the breathing sound, observing the chest movements, placing a piece of metal (glass) beneath the nose, and observing the steam from breath humidity, etc. Now there are clinical methods such as pulse oximetry, which is not flexible due to low accuracy and lack of portability. Hence, in recent years, it has been necessary to devise a highly reliable, flexible, and sensitive sensor. The device should have precise sensor dimensions, optimum power consumption and convenience for patients use. Therefore, different piezoelectric material performances, and the mathematical characterizations have been considered for the design. Various layers such as Polyvinylidene Fluoride (PVDF), Copper [7], and Flame Retardant-4 (FR-4) [29], are used to design the piezoelectric sensors and beams. These layers can be exploited for protecting the sensors and tuning the resonance frequency.

There have been many complaints from the patients about the convenience of wearing belts for breath monitoring. Therefore, PVDF has been used due to its high sensitivity, consistent flexibility with the human body and a lightweight [8].

Sensor position to perfectly record the breathing signals, as well as wearing convenience are very important. In this work, a triangle-paired shape sensor, with three stacked layers of two different materials are used for the sensor fabrication. The structure is capable of producing the breath signals through the chest displacement according to the direct piezoelectric effect. The piezoelectric sensor generates electrical breathing signal that is amplified by a charge amplifier and a following filter is used to cancel noise.

This paper is organized as follows. Section 2 is a review of the previous works. The mathematical concepts of the sensor are addressed in Section 3. Section 4 describes sensor structure and fabrication process. Sensor model and the interface circuit are explained in Section 5. Discussions are in Section 6 and concluding remarks are at the end.

* Corresponding author.
E-mail address: a_hassanzadeh@sbu.ac.ir (A. Hassanzadeh).

https://doi.org/10.1016/j.sbsr.2020.100378
Received 28 June 2020; Received in revised form 12 September 2020; Accepted 28 September 2020
Available online 03 October 2020

2. Related work

Ono et al. have reported a unimorph-type bending sensor beneath the nose and on top of the mouth. By using the piezoelectric theory and Bernoullis law he showed that the nose air speed is proportional to the square of the output voltage for the piezoelectric sensor [9].

$$V_o = \left\{ \frac{4s_{11}^p L(AB+1)}{3Wt_p AB(B+1)} \rho S \right\} {v_f}^2 \tag{1}$$

$$A = \frac{E_m}{E_p},\ B = \frac{h_m}{h_p} \tag{2}$$

where L and W are the sensor length and width, E_m and h_m are Young modulus and the thickness of the substrate, and E_p and h_p are Young modulus and the thickness of the piezoelectric, respectively. ρ is the air density and S is the area of the sensor where the airflow is applied. In Ono's work, a breathing simulator as an air flow chamber with an area of $242mm^2$ has been used, inside which the sensor is positioned. The substrate is metal type material.

A sensor based on curved PVDF for monitoring the heart and breathing is designed as an ellipse shape, whereas the curved PVDF film is placed in the middle layer between the PDMS and Mylar (BoPET) layers. Two electrodes on the top and bottom of the PVDF film are used to transfer the signal. A voltage amplifier has been used to amplify signals and a low pass filter is mounted to record the breathing signals. The sensor has the features of small dimensions, light weight, low cost, and portability. It has been shown that when the PVDF layer bends significantly, it increases the diagnosing breathing signal compared to the flat mode [10]. After capturing the breathing signals, a charge amplifier amplifies the signal from the piezo sensor. Mahbub in 2017 used two piezoelectric electrodes on the chest for detecting the vibration. A CMOS IC had been fabricated in 130 nm technology for signal conditioning and sending data to a monitoring system. The device can be placed in a coat or a jacket as shown in Fig. 1 [11].

The sensor charge is converted to voltage and amplified by a charge amplifier and converted to digital using an ADC. The direct piezoelectric effect will be used in the forces and breathing frequency simulations. This means that the applied force on the sensor surface (PVDF material) polarizes the molecules of the piezoelectric material and creates charge at the output [30]. Using a monitoring belt with the PVDF film consisting of a piezoelectric converter and a harvester circuit, Abdi has reported the atmospheric pressure on the abdomen surface between 3.4 and 4.9 kPa in the breathing frequency of 0.35 Hz (in practice and sport mode), and between 3.2 and 4.2 kPa in the breathing frequency of 0.25 Hz (in the rest mode). He has shown that the bent PVDF film diagnoses better the breathing signals [12]. In a multi-arc sensor, the curvature of the sensor structure plays a key role in generating voltage in the piezoelectric material [28].

In the energy collector piezoelectric beam, Asan et al. by comparing the three modes of triangular, trapezoidal, and rectangular shapes have shown that the voltage generated in the piezoelectric beam is highly dependent on the geometry and the size of the piezoelectric material [7]. Hence, it requires the definition of an optimal form for the energy configuration. Triangular shape is proposed to reach the maximum voltage due to the fixed strain along the beam [7]. Kia et al. have shown the use of multiple triangular shapes is an optimum design for energy harvesting applications and wireless sensor networks [29]. In this work, Bernoullis law is used in the piezoelectric beams, and the beams are combined for breath monitoring. By simulating a triangular beam including two layer piezo and insulation, by decreasing the thickness of piezoelectric layer, a higher voltage is generated at the output. Therefore, choosing the beam thickness is completely dependent on the manufacturing technology. Also, increasing the length and width of the beam is directly proportional to the voltage amplitude. On the other hand, the proportionality of the voltage growing speed to the width is lower than to the length. Thus, higher voltage means more displacement, and this is used for better monitoring.

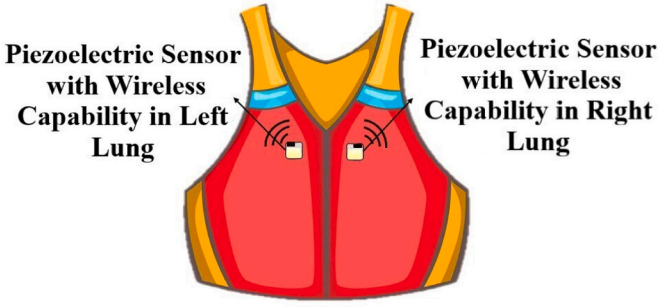

Fig. 1. Sensor placement in the jacket [11].

3. Piezoelectric cantilever beam equation

The motion equation, $f_0(x,t)$ along a beam is obtained from the Euler-Bernoulli beam theory. For a steady beam under free vibration [13,14]:

$$EI\frac{\partial^4 z(x,t)}{\partial x^4} + m\frac{\partial^2 z(x,t)}{\partial t^2} = f_0(x,t) \tag{3}$$

where EI is the bending stiffness, m is the mass per unit length, and $z(x,t)$ is the lateral displacement in the neutral axis (at point x and the time t) due to the bending. $z(x,t)$ can also be shown as follows:

$$z(x,t) = z_b(x,t) + z_{rel}(x,t) \tag{4}$$

where $z_b(x,t)$ is the beam base displacement, and $z_{rel}(x,t)$ is the beam transverse displacement. Eq. (5) shows the natural frequencies for a rectangular beam. It is the mode shape of the beam in the k-th vibration mode, which is the system natural frequency, by which β_k and λ_k are as follows:

$$w_k(x) = \sin\left(\frac{\lambda_k}{L}x\right) - \sinh\left(\frac{\lambda_k}{L}x\right) + \beta_k\left[\cos\left(\frac{\lambda_k}{L}x\right) - \cosh\left(\frac{\lambda_k}{L}x\right)\right] \tag{5}$$

Nevertheless β_k:

$$\beta_k = \frac{-\cos\lambda_k - \cosh\lambda_k}{-\sin\lambda_k + \sinh\lambda_k} \tag{6}$$

In this section, the natural frequencies of the triangular beam, which differs from the rectangular beam is approximated. The Rayleigh-Ritz method is used with a function of the widths ratio [7,14]. Because of the triangular shape, the two widths ratio is zero. Then, the width function for the triangular shape is as follows:

$$B(x) = \frac{B(0)}{L}(L - x) \tag{7}$$

where $B(0)$ is the width of the fixed part (base) of the triangle. Therefore, (5) will be rewritten as follows:

$$w_k(x,t) = \left[\sin\left(\frac{\lambda_k}{L}x\right) - \sinh\left(\frac{\lambda_k}{L}x\right) + \beta_k\left[\cos\left(\frac{\lambda_k}{L}x\right) - \cosh\left(\frac{\lambda_k}{L}x\right)\right]\right]\sin(\omega t + \alpha) \tag{8}$$

where α is a constant, ω is the angular frequency and t shows the time. λ is equal to the coefficient of stiffness (EI) and mass (m) is a positive coefficient. The kinetic energy of the system is obtained from the following relation:

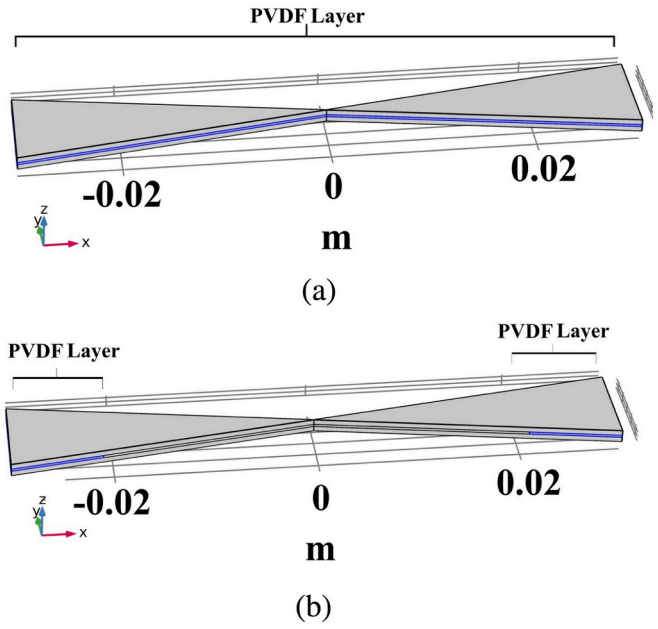

Fig. 2. The proposed piezoelectric sensor for breath monitoring (a) piezoelectric layer covering all the surface. (b) piezoelectric layer covering the surface partially.

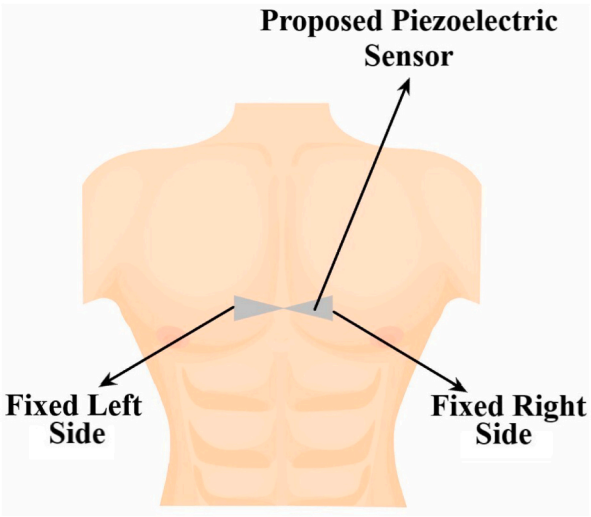

Fig. 3. Sensor position on the patient's chest.

$$T = \int_0^L \frac{1}{2}(\rho_b h_b + \rho_p h_p) B(x) dx \left(\frac{\partial z(x,t)}{\partial x^2}\right)^2 dx \tag{9}$$

The potential energy is determined by the following equation:

$$U = \int_0^L \frac{1}{2} EI(x) \left(\frac{\partial^2 w_k(x,t)}{\partial t}\right) \tag{10}$$

Then, according to the conservation law, the natural frequency in (11) is obtained:

$$w_k = \sqrt{\frac{\int_0^L B(x)\left[-\sin\left(\frac{\lambda_k}{L}x\right) - \sinh\left(\frac{\lambda_k}{L}x\right) + \beta_k\left[-\cos\left(\frac{\lambda_k}{L}x\right) - \cosh\left(\frac{\lambda_k}{L}x\right)\right]\right]^2 dx}{(\rho_b h_b + \rho_p h_p)}}{\frac{\int_0^L B(x)\left[\sin\left(\frac{\lambda_k}{L}x\right) - \sinh\left(\frac{\lambda_k}{L}x\right) + \beta_k\left[-\cos\left(\frac{\lambda_k}{L}x\right) - \cosh\left(\frac{\lambda_k}{L}x\right)\right]\right]^2 dx}{\left[\left(\frac{\lambda_k}{L}\right)^4 Y_b\left(\frac{\lambda_b}{12}\right) + \frac{Y_p}{3}\left(\left(\frac{h_b}{2} + h_p\right)^3 - \frac{h_b^3}{8}\right)\right]}} \tag{11}$$

Natural frequency in (11) shows the vibration mode of the beam and its dependence on the mechanical dimention of the beam and properties of layers. Y_b and Y_p are the Young's modulus of the substrate (PDMS) and piezoelectric material (PVDF), respectively. Euler-Bernoulli

Table 1
Material specifications PVDF and PDMS layer used for simulation.

Layer parameter	PDMS layer (b)	PVDF layer (p)
Thickness, h [μm]	500	250
Length, L [cm]	3	3
Width, B [cm]	1	1
Mass density, ρ [kg/m^3]	970	1780
Young modulus, Y [kPa]	750	2.1e6
Relative permitivity, ε	2.75	7.74

Table 2
The mode shapes (resonant frequencies) 1 to 3 for both Figs. 2 a and b.

Mode Shapes	Mode Shape1	Mode Shape 2	Mode Shape 3
Fig. 2 a	70.34 Hz	151.16 Hz	298.15 Hz
Fig. 2 b	26.159 Hz	54.041 Hz	101.93 Hz

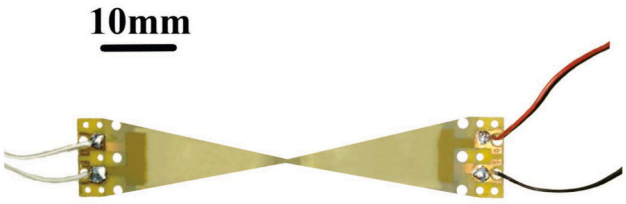

Fig. 4. Fabricated respiration monitoring sensor.

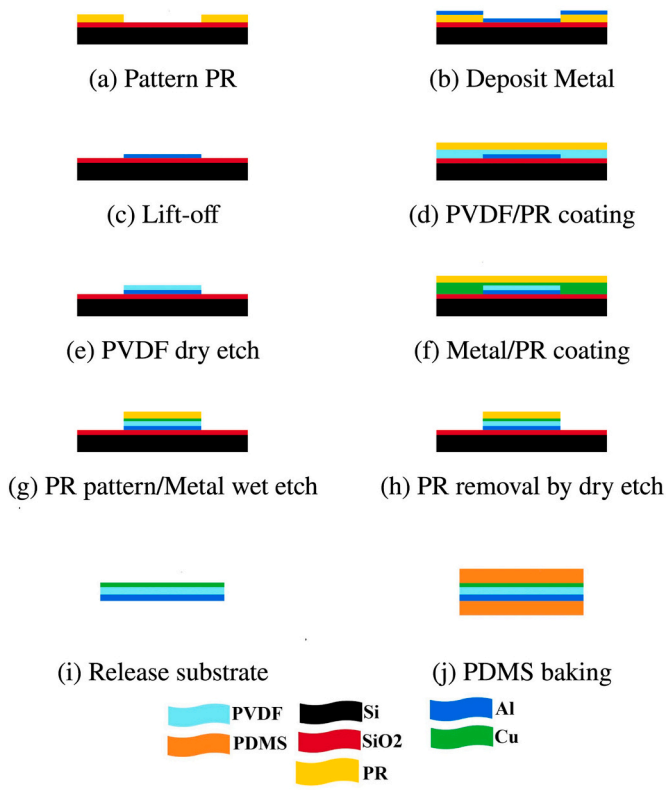

Fig. 5. Fabrication process.

equations have been used to determine the mode shapes and find the natural frequency of the sensor in the next section.

4. The proposed piezoelectric sensor design

In the introduction, it has been shown that using a triangular shape for the piezoelectric beam increases the displacement and stretch, and subsequently generates higher voltage [4]. For this reason, a vertex-attached triangular-paired shape has been used, which the larger widths are in a fixed position as shown in Fig. 2.

Two different materials of PDMS and PVDF are used in the sensor fabrication. In Fig. 2 b, PVDF only is placed on the rear part of the fixed beams that reduces the resonant frequency of the system. To further decrease the resonance frequency, a tip mass can be used that has applications in energy harvesting too [15,16]. The tip mass has not been used because it increases the sensor weight. Each triangle tip is placed on the patients chest. The tip vibrations because of breathing pressure generate a voltage on the sensor surface. This can be used to collect energy and monitor the respiratory patients. It has been shown that the characteristics of the PVDF layer can change by humidity [8]. Because of humidity of human body skin from sweat and other conditions, a PDMS layer must be used as an insulator and confiner for the electronic sensors. Furthermore, PDMS materials are environmental friendly and have many applications in biology and biomedicine systems [17–19].

The sensor position for the highest sensitivity for breath monitoring is very important as shown in Fig. 3. The tape has a minor effect on the output signal of the piezoelectric sensor, because it has the same displacement as the piezoelectric transducer. An experimental setup shows negligible effect on the signal output. Minor signal attenuation because of the tape can be compensated using the amplifier stage.

The position of the sensor on the patient's chest affects the amplitude of the output signal. The upper side of the chest has smaller movement and the lower has larger displacement and gradually decreases. The best position for the larger displacement has been investigated in reference [27]. A rule of thumb is that by looking at the patients chest horizontally, and find the area that has the highest movement. Attach the sensor horizontally on that area as shown in Fig. 3.

PDMS has proper elasticity and deformation along with the PVDF material. It has been shown that using a softer material increases the signal magnitude by three times [10]. The sensor signal is amplified using a low power amplifier followed by a low pass filter with a cut-off frequency of 5 Hz. The filter removes unwanted and out of band signals. Patient movement or shivering creates higher frequency noise that is out of the filter passband. The breathing rate falls between 0.1 and 0.5 Hz and is in the passband of the filter and no information of the signal will be lost. This has been confirmed by the simulation and experiment. While capturing the respiratory signals, it is possible that heart signals interfere with the breathing data. To avoid this, a band-pass filter in a range from 0.8 to 2 Hz, which is the heart beat overlay zone, can be used to protect data [20]. Additionally, to record the breathing signals, it is necessary to use a band-pass filter tuned in the range of 0.1 to 0.5 Hz [21].

The material specifications and sizes for both layers are specified. For the two shapes with the designed resonant frequencies and dimensions are listed in Table 1 and Table 2. It can be seen from the

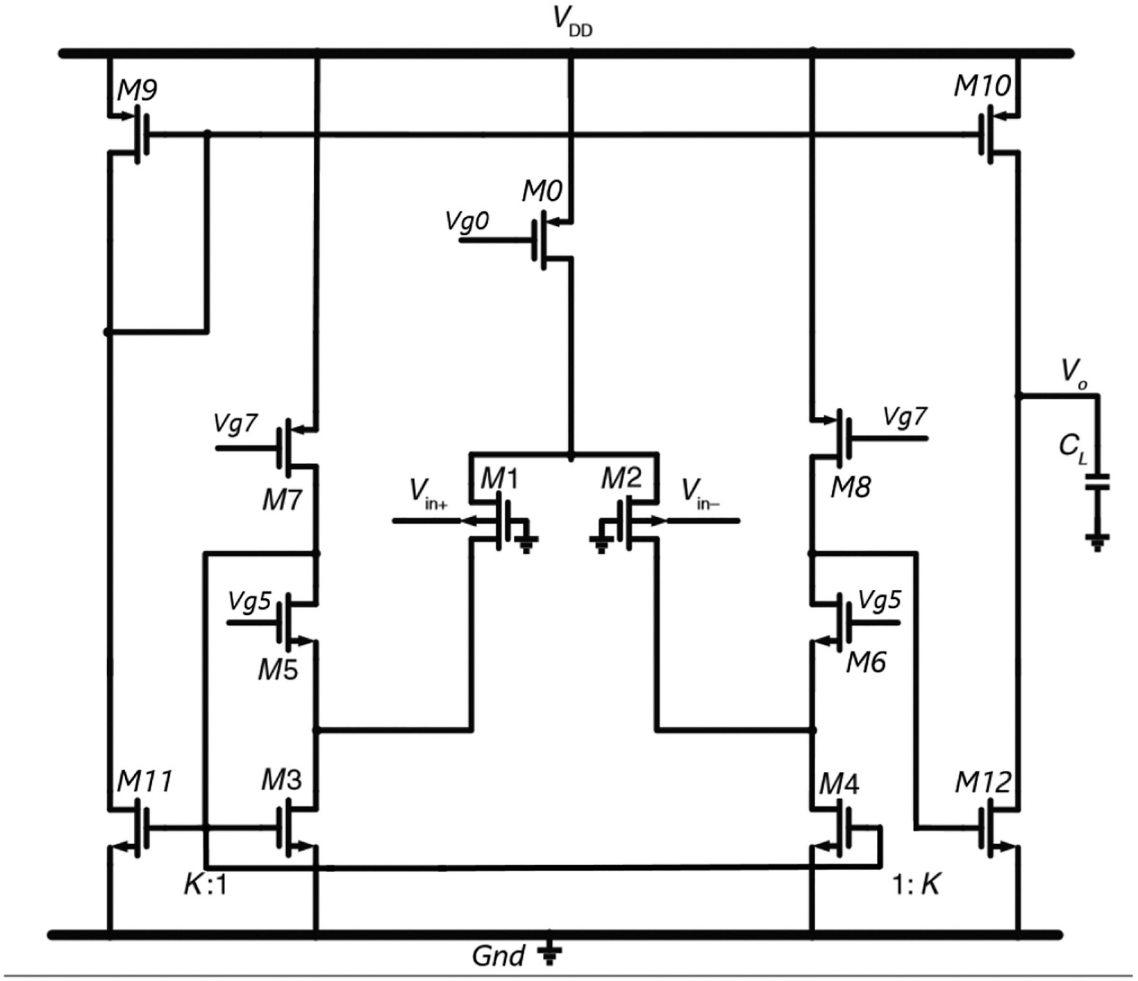

Fig. 6. Bulk-driven OTA (K = 3).

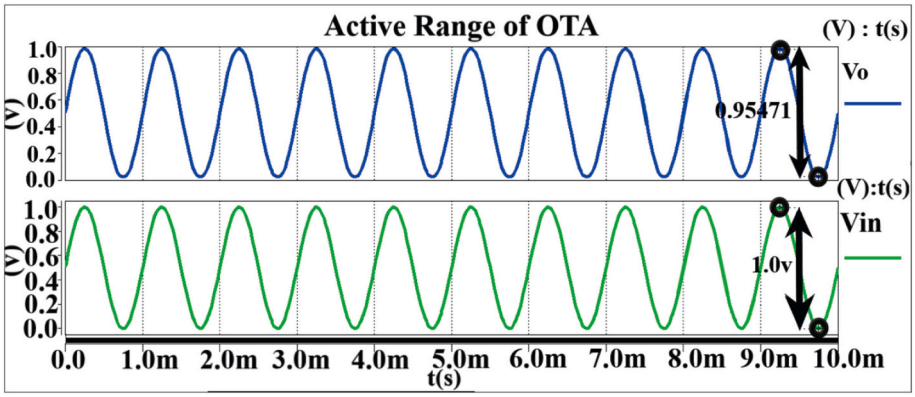

Fig. 7. Dynamic range of the input and output of the OTA.

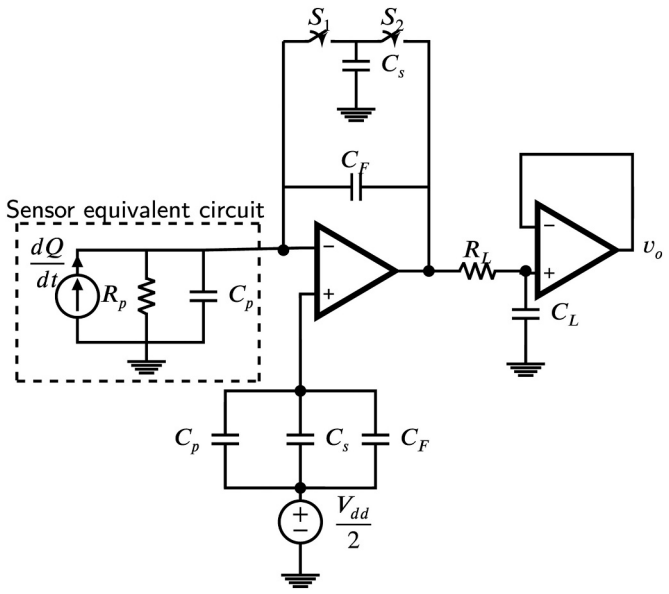

Fig. 8. Proposed interface circuit for the breathing sensor.

Table 1 that by placing the PVDF layer on the rear part of the triangular beam (Fig. 2 b), the resonant frequency is reduced by more than 60%.

In this work, the sensor has been fabricated using a sandwich method, where the piezoelectric layer is in between two polymer layers [22]. The process starts on a silicon substrate. First, a photoresist layer is spin-coated on the substrate and patterned. An Aluminum layer (200 nm) is coated using physical vapor deposition (PVD), and the extra metal is removed using lift-off process (Fig. 5 a, b, c). PVDF is spin-coated on top and is covered with a photoresist. PVDF thickness can be adjusted by the speed of spinning. For example, a 2000 rpm rotation speed for 30s, gets 1μm thickness. The patterned PVDF is etched using an RIE process (Fig. 5 d, e). The final layer of Copper with 120 nm thickness is patterned using photoresist and wet etching (Fig. 5 f, g, h). After the device is released from the substrate, PDMS is spin-coated on both sides of the device and baked for hardening. PDMS thickness is adjusted using the spin speed (Fig. 5 i, j). The top view of the fabricated triangular-paired sensor with both ends fixed is shown in Fig. 4.

5. Interface circuit

The interface circuit can be used for the sensor for amplification and filtering purposes. The equivalent circuit for the piezoelectric sensor is a current source with a parallel capacitor and resistor. The source signal generates charge pulses that should be amplified in the next stage. The equivalent parallel capacitor is determined by the size of the sensor and the dielectric coefficient of PVDF. Charge amplifiers have been used for neural recording amplification, touch-pad sense system and piezoelectric amplifiers [23–25]. The charge amplifier amplifies the charge signal and generates a voltage signal at the output [26]. An amplifier with a parallel resistor-capacitor feedback has been used to amplify charge on the piezoelectric plates. The main amplifier consists of a low power bulk-driven Operational Transconductance Amplifier (OTA) as shown in Fig. 6. The piezoelectric model has a parallel resistor with the capacitor. The value of the resistor for the designed sensor is in the range of Giga Ohm and it has negligible effect on the circuit performance.

The OTA has about 1.019 MHz bandwidth and 42 μW of power consumption with 0.4 pF load capacitance. Transistor sizes of the amplifier are shown in Table 3. After the charge amplifier, a low pass filter

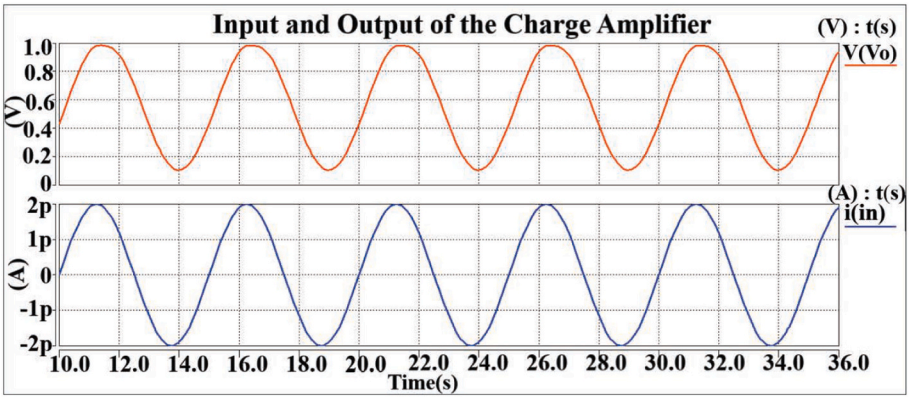

Fig. 9. Input and output waveform of the charge amplifier.

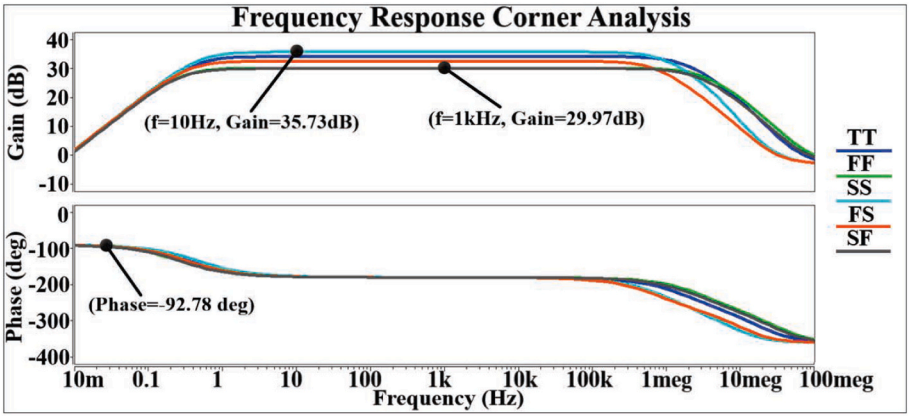

Fig. 10. Corner analysis of the amplifier frequency response.

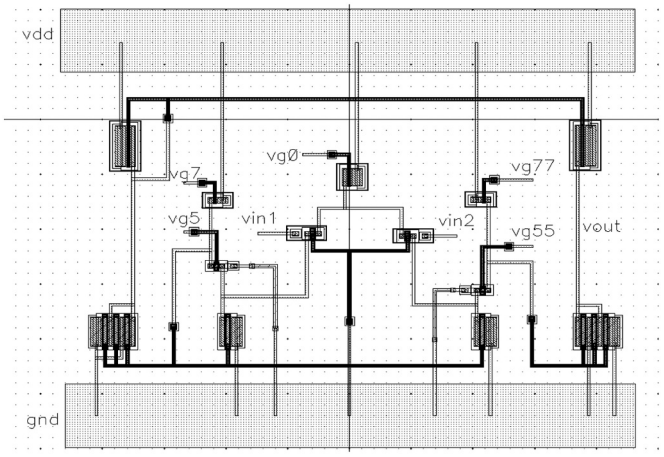

Fig. 11. Layout of the OTA.

is used to filter out unwanted signals. To reduce the power consumption of the amplifier 1 Vsupply voltage has been used. The maximum output voltage of the piezoelectric transducer is smaller than the supply voltage and stays within the acceptable input voltage range of the amplifier. The dynamic range of the amplifier for the breath signal is shown in Fig. 7.

The proposed interface circuit for the breathing sensor is shown in Fig. 8.

To implement the large feedback resistor a switched capacitor circuit with non-overlapping clocks has been used. The resistor value can be estimated using (12) with a 50fF capacitor and 2 kHz clock frequency.

$$R_f = \frac{1}{C_s f_s} \tag{12}$$

Balanced impedances have been used in the inverting and non-inverting terminals of the charge amplifier to reduce any offset voltage and noise at the inputs. The piezoelectric capacitance is 80.7 pF and the feedback capacitor is 1 pF. The low pass filter resistor and capacitor are 90 M Ohm and 2.2 nF respectively.

Fig. 9 shows a single tone current signal of 0.25 Hz, which represents piezoelectric output charge that is amplified and converted to a voltage output signal using the charge amplifier. In order to symmetrically amplify the signal output, DC offset of the amplifier has been set to half of the supply voltage, about 0.4–0.5 V. This offset is intentional and is different from the small random offset of the amplifier inputs because of component mismatch. Charge amplifier corner

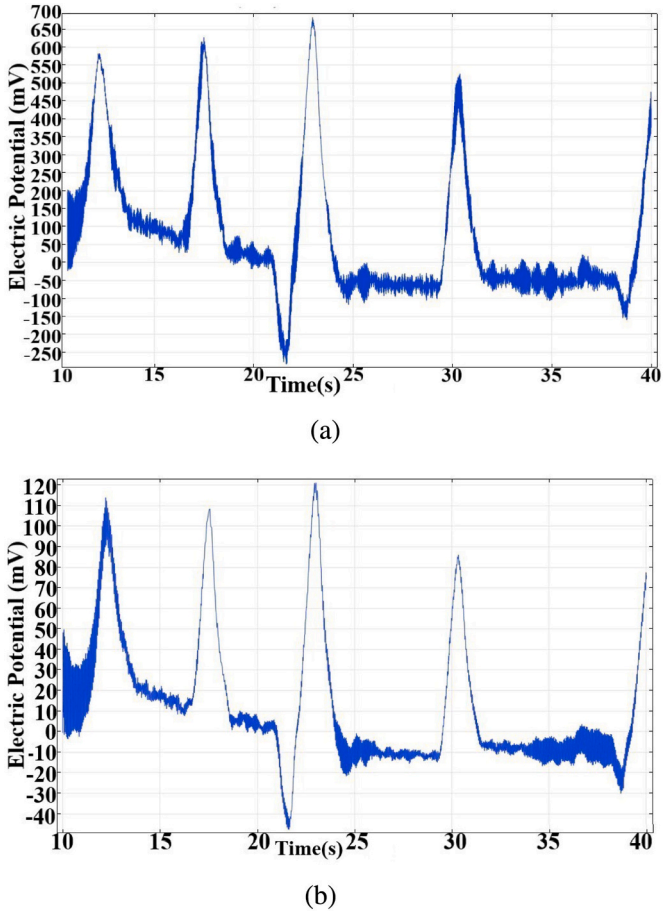

Fig. 12. The acquired breathing signals (a) Breathing signals recorded by the sensor of Fig. 2 a. (b) Breathing signals recorded by the sensor of Fig. 2 b.

analysis for (FF, FS, SF, SS) transistors are shown in Fig. 10 that shows robust performance of the designed amplifier. The worst case phase margin is about 88 degrees. Fig. 10 shows process variation of the technology and its effect on the amplifier frequency and phase response. The plot shows that the amplifier performance meets the requirement for the gain and stability criteria.

The OTA layout has been simulated using Cadence software as shown in Fig. 11.

To cancel the loading effect on the piezoelectric sensor and amplify

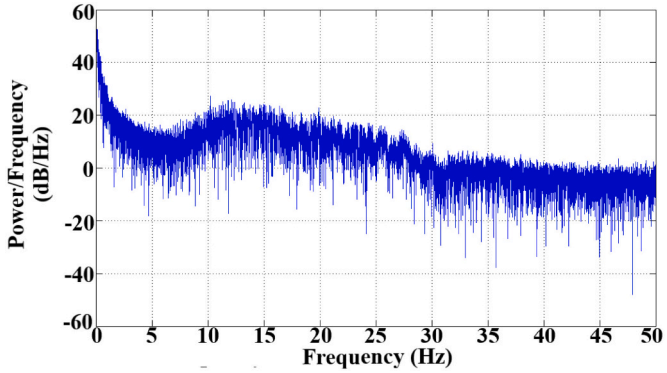

Fig. 13. Periodogram power spectral density of breathing signals.

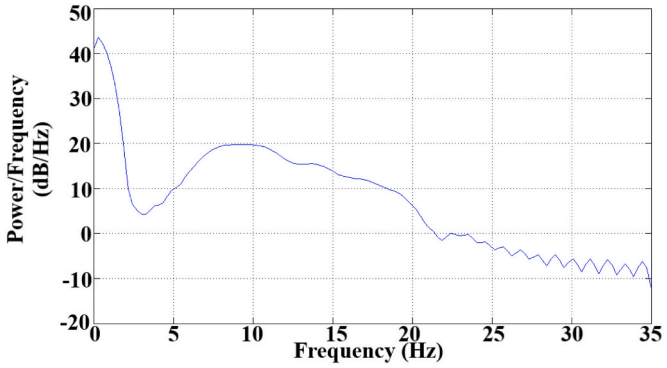

Fig. 14. Welch (noiseless) power spectral density of breathing signals.

weak vibrations, signal conditioning circuits are required. The first stage is an Operational Transconductance Amplifier (OTA) and the next stage is a low pass filter. The amplifier amplifies the transducer signal and prepares it for the next stage of Analog to Digital Converter (ADC).

6. Analysis and discussion

The proposed respiration sensor consists of a cantilever beam structure and the piezoelectric to improve the performance and increase the sensitivity of the sensor. The low cost sensor can be used by individuals to continuously monitor breath rate while staying at home during COVID-19 pandemic. The human chest displacement amount where the sensor is placed has been reported to be 4–12 mm [27]. The output signals of the two sensors have been recorded and are shown in Fig. 12 a, b. The record length is about 150 s and the output has been shown for 10 to 40 s.

As shown in Fig. 12 a, the maximum output voltage for normal adult breathing is about 650 mV that decreases to 120 mV for the second sensor in Fig. 12 b. The low output voltage of the second sensor is because of the smaller amount of the PVDF material used, which reduce sensor cost. The low output voltage can be compensated by the proposed charge amplifier gain.

Clinical research on the human body shows that the breathing rate ranges from 0.2 Hz when sleeping, 0.3 Hz in normal condition and about 0.5 Hz after workout. The frequency range is fully supported and amplified by the interface circuits. Shivering and sudden patient movements have higher frequency components that are filtered out using the existing low pass filter.

The Power Spectral Density (PSD) of the output signal has been shown in Figs. 13 and 14 using Periodogram and Welch in MATLAB. As it is expected, the breath signal power is at 0.2 Hz and at its maximum value is 42 dB/Hz. The result fully matches the breath signal spectrum.

Table 4 compares performance of the proposed sensor and the previous reports. Sensor position, physical shape, interface circuit, piezo material and other parameters have been listed. Since an optimized combination of a cantilever structure and piezoelectric material has been used, the sensitivity and output signal of the sensor has increased compared to the previous reports. The sensors fully cover the breathing signal frequency range. The sensor shape has a large impact on the sensor sensitivity and output signal. The second sensor has lower fabrication cost.

Fig. 15 shows the input and output waveform of the low pass filter. High frequency components and noise have been canceled out. The required attenuation can be altered using higher order filters.

In Fig. 16 the piezoelectric sensor has been simulated using COMSOL software for the temperature range of 20–50, which is a typical range of operation of a live person. Simulation results show that the output signal amplitude is slightly affected by the temperature change. The output voltage temperature coefficient is about 1.6 mV/°C. The piezoelectric material used in this sensor is PVDF, which is an

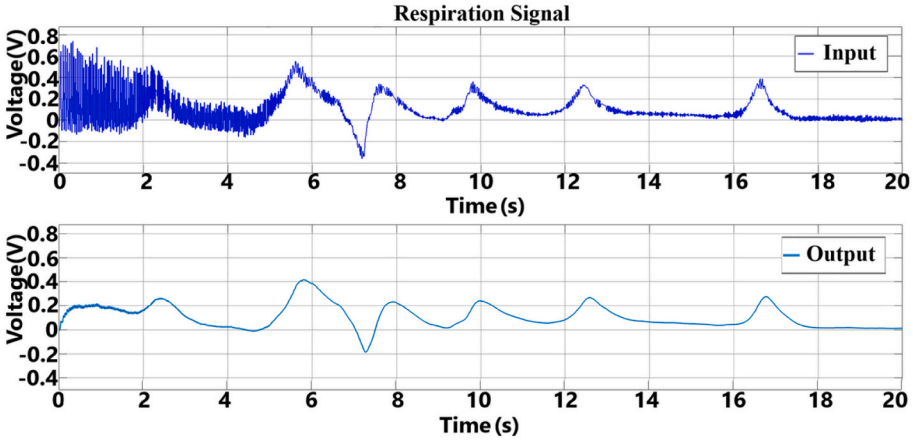

Fig. 15. Respiration signal before and after low pass filter.

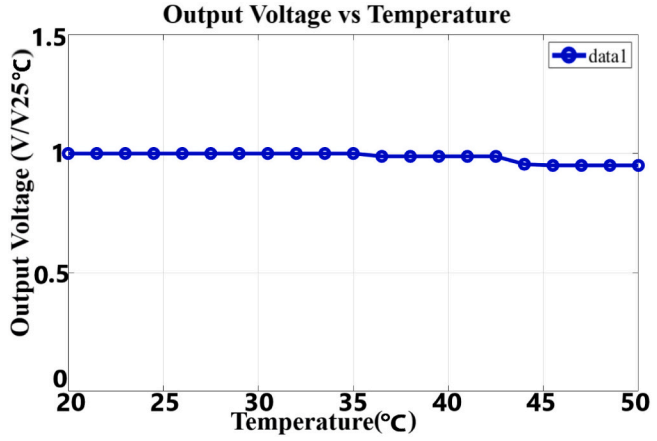

Fig. 16. Temperature analysis for the proposed sensor.

Table 3
Transistor sizes and area of the interface circuit.

Transistors	Width[μm]	Length[μm]	Fingers(K)
$M1$	0.41	0.36	1
$M2$	0.41	0.36	1
$M3$	2.65	0.36	1
$M4$	2.65	0.36	1
$M5$	0.3	0.36	1
$M6$	0.3	0.36	1
$M7$	0.52	0.18	1
$M8$	0.52	0.18	1
$M9$	3.7	0.18	1
$M10$	3.7	0.18	1
$M11$	2.65	0.36	3
$M12$	2.65	0.36	3
$M0$	1.6	0.18	1

Area of the interface circuit $= 0.024mm^2$

expensive material. The amount of PVDF affects the sensor price. In references [10, 12, 28], a large area of PVDF has been used, but in this design, a smaller area of PVDF has been used. Smaller piezo material will produce a smaller output signal that has been compensated using the attached charge amplifier.

7. Conclusion

A low cost, low frequency triangular shape piezoelectric sensor has been designed for continuous breath monitoring applications. The sensor consists of a PVDF layer coated with PDMS to prevent the moisture and the human bodys sweat. The output voltage to the input pressure ratio is about 41% higher in the triangular shape compared to the rectangular shape.

The equivalent sensor model has been used for the simulations and the sensor output charge is amplified using a low power charge amplifier. The output breathing signal can reach 650 mV by the maximum chest movement in typical mode, and has a 42 dB/Hz power at 0.2 Hz frequency. The output low-pass filter cancels high frequency noise and the mechanical movement noise. The low cost sensor can be used for at home breath monitoring of COVID-19 virus patients.

Author statement

Thank you very much for all the useful comments on our research paper “Design of a Low Cost, Double Triangle, Piezoelectric Sensor for Respiratory Monitoring Applications “. The reviewers' suggestions have improved the quality of our paper. I have responded and addressed all the questions of the reviewers in the attached reviewer's response file. All the changes have been highlighted in the text. The revised version and highlighted corrections have been uploaded. Please let me know if you have any other questions.

Amir Panahi was born in Baneh city, Iran in 1994. He received the B·S. degree in electrical engineering from Urmia University, Urmia, Iran, in 2017 and the M.S. degree in integrated circuit engineering from Shahid Beheshti University, Tehran, Iran, in 2020. His research interests are related to sensor technology, piezoelectric material biosensors, bioengineering system, piezoelectric beams vibration, energy harvesting and interface circuit of these structures to electrical modeling. Amir has been working on biomedical sensors and systems, since 2017.

A. Hassanzadeh received his MSc and PhD from the University of Alabama in Huntsville, USA in 2008 and 2011 respectively. He is currently an assistant professor at EE department of the SBU. His research interests include analog and low power IC design, sensors and instrumentation.

Ali Moulavi was born in Mashhad, Iran, in 1993. he received the B.Sc. degree in electrical engineering from the *Imam* Reza International University, Mashhad, Iran, in 2017, the M.Sc. degree in Integrated Circuits from the Shahid Beheshti University, Tehran, Iran in 2020. Ali has been working on sensors and biosensors since 2018. His research interest includes analog circuit design for sensor and biosensor systems, wireless systems, MEMS applications, and energy harvesting systems.

Declaration of Competing Interest

The authors declare that they have no known competing financial interests or personal relationships that could have appeared to influence the work reported in this paper.

Table 4
Comparison table.

Reference	Ono [9]	Chiu [10]	Mahbub [11]	Abdi [12]	Xin [28]	This work
Methods	Air flow	Chest wall	jacket at chest	Abdomen	Abdomen belt	Chest wall
Sensor shapes	Unimorph bending	Curved ellipse	–	Belt	Multi-arch	Triangular-paired
Interface	–	Voltage amplifier	Charge amplifier	Harvester circuit	Charge amplifier	Charge amplifier
Piezoelectric material	PZT	PVDF	PVDF	PVDF	PVDF	PVDF
Max. voltage	1 V	500 mV	500 mV	210 mV	500 mV	650 mV

References

[1] Miemss.org, Maryland EMS. [online], (2020) Available at: < http://www.miems-s.org/ > [Accessed 8 August 2020].
[2] M.A. Cretikos, R. Bellomo, K. Hillman, J. Chen, S. Finfer, A. Flabouris, Respiratory rate: the neglected vital sign, Med. J. Aust. 188 (11) (2008) 657659.
[3] K. Hillman, P. Bristow, T. Chey, K. Daffurn, T. Jacques, S. Norman, G. Bishop, G. Simmons, Antecedents to hospital deaths, Intern. Med. J. 31 (6) (2001) 343348.
[4] A.M. Berzlanovich, B. Fazeny-Dlorner, T. Waldhoer, P. Fasching, W. Keil, Foreign body asphyxia: a preventable cause of death in the elderly, Am. J. Prev. Med. 28 (1) (2005) 6569.
[5] A. Lurie, Obstructive sleep apnea in adults: epidemiology, clinical presentation, and treatment options, Obstructive Sleep Apnea in Adults, vol. 46, Karger Publishers, 2011, p. 142.
[6] F. Pan, T. Ye, P. Sun, S. Gui, B. Liang, L. Li, D. Zheng, J. Wang, R.L. Hesketh, L. Yang, et al., Time course of lung changes on chest ct during recovery from 2019 novel coronavirus (covid-19) pneumonia, Radiology (2020) 200370.
[7] A.G. Muthalif, N.D. Nordin, Optimal piezoelectric beam shape for single and broadband vibration energy harvesting: modeling, simulation and experimental results, Mech. Syst. Signal Process. 54 (2015) 417426.
[8] S. Rajala, J. Lekkala, Film-type sensor materials pvdf and em in measurement of cardiorespiratory signalsa review, IEEE Sensors J. 12 (3) (2010) 439446.
[9] Y. Ono, D. Mohamed, M. Kobayashi, C.-K. Jen, Piezoelectric membrane sensor and technique for breathing monitoring, 2008IEEE Ultrasonics Symposium, IEEE, 2008, p. 795798.
[10] Y.-Y. Chiu, W.-Y. Lin, H.-Y. Wang, S.-B. Huang, M.-H. Wu, Development of a piezoelectric polyvinylidene uoride (pvdf) polymer-based sensor patch for simultaneous heartbeat and respiration monitoring, Sensors Actuators A Phys. 189 (2013) 328334.
[11] I. Mahbub, S.A. Pullano, H. Wang, S.K. Islam, A.S. Fiorillo, G. To, M. Mahfouz, A low-power wireless piezoelectric sensorbased respiration monitoring system realized in cmos process, IEEE Sensors J. 17 (6) (2017) 18581864.
[12] H. Abdi, N. Mohajer, S. Nahavandi, Human passive motions and a user-friendly energy harvesting system, J. Intell. Mater. Syst. Struct. 25 (8) (2014) 923936.
[13] A.D. Dimarogonas, Vibration for Engineers, Prentice Hall, 1996.
[14] K. Yang, Z. Li, Y. Jing, D. Chen, T. Ye, Research on the resonant frequency formula of v-shaped cantilevers, 2009 4th IEEE International Conference on Nano/Micro Engineered and Molecular Systems, IEEE, 2009, p. 5962.
[15] J. Ajitsaria, S.-Y. Choe, D. Shen, D. Kim, Modeling and analysis of a bimorph piezoelectric cantilever beam for voltage generation, Smart Mater. Struct. 16 (2) (2007) 447.
[16] M. Fakhzan, A.G. Muthalif, Harvesting vibration energy using piezoelectric material: Modeling, simulation and experimental verications, Mechatronics 23 (1) (2013) 6166.
[17] J. Park, H.S. Kim, A. Han, Micropatterning of poly (dimethylsiloxane) using a photoresist lift-off technique for selective electrical insulation of microelectrode arrays, J. Micromech. Microeng. 19 (6) (2009) 065016.
[18] M.A. Sherman, J.P. Kennedy, D.L. Ely, D. Smith, Novel polyisobutylene/poly-dimethylsiloxane bicomponent networks: Iii. tissue compatibility, J. Biomater. Sci. Polym. Ed. 10 (3) (1999) 259269.
[19] J.N. Lee, X. Jiang, D. Ryan, G.M. Whitesides, Compatibility of mammalian cells on surfaces of poly (dimethylsiloxane), Langmuir 20 (26) (2004) 1168411691.
[20] D.H. Spodick, Normal Sinus Heart Rate: Sinus Tachycardia and Sinus Bradycardia Redened, (1992).
[21] L. Sherwood, Fundamentals of physiology: A human perspective, Thomson brooks, Belmont, Ca, 2006.
[22] T. Sharma, S.-S. Je, B. Gill, J.X. Zhang, Patterning piezoelectric thin lm pvdftrfe based pressure sensor for catheter application, Sensors Actuators A Phys. 177 (2012) pp. 87 92.
[23] L. Pinna, M. Valle, Charge amplier design methodology for pvdfbased tactile sensors, J. Circu. Syst. Comput. 22 (08) (2013) 1350066.
[24] P. Kmon, P. Gryboś, Energy efcient low-noise multichannel neural amplier in submicron cmos process, IEEE Transactions on Circuits and Systems I: Regular Papers, 60 2013 no. 7. pp. 1764 1775.
[25] T. Starecki, Analog front-end circuitry in piezoelectric and microphone detection of photoacoustic signals, Int. J. Thermophys. 35 (11) (2014) 21242139.
[26] I. Mahbub, S. Shamsir, S.A. Pullano, A.S. Fiorillo, S.K. Islam, Design of a charge amplier for a low-power respirationmonitoring system, IET Circu. Devi.Syst. 13 (4) (2019) 499503.
[27] G. Shaq, K.C. Veluvolu, Surface chest motion decomposition for cardiovascular monitoring, Sci. Report. 4 (2014) 5093.
[28] Yi Xin, et al., Development of respiratory monitoring and actions recognition based on a pressure sensor with multi-arch structures, Sensors Actuators A Phys. 296 (2019) 357–366.
[29] G. Kia, A. Hassanzadeh, HYREP: a hybrid low-power protocol for wireless sensor networks, international journal of engineering (IJE), IJE Trans. A: Basics 32 (4) (April 2019) 519–527.
[30] R.S. Dahiya, M. Valle, Appendix A Fundamentals of piezoelectricity, de Robotic Tactile Sensing, Springer, 2013.